The penetration of sunflower root tissues by the parasitic plant Orobanche cumana is intracellular

Marie-Christine Auriac, Caitlin Griffiths, Alexandre Robin-Soriano, Alexandra Legendre, Marie-Claude Boniface, Stéphane Muños, Joëlle Fournier, Mireille Chabaud

Title

The penetration of sunflower root tissues by the parasitic plant *Orobanche cumana* Wallr. is intracellular.

Auriac MC, Griffiths C, Robin-Soriano A, Legendre A, Boniface MC, Muños S, Fournier J, and Chabaud M.

Key message

Combination of *in vivo* confocal, large field and transmission electron microscopy approaches revealed how intimate the relationship between the parasitic plant broomrape (*Orobanche cumana* Wallr.) and its sunflower host (*Helianthus annus* L.) is at very early stages of their interaction.

Key words

Live-cell imaging, parasitic plant, *Orobanche cumana*, *Helianthus annuus* L., plant-plant interaction.

Introduction

Sunflower broomrape (*Orobanche cumana*) is one of the main pests for sunflower crops. This holo-parasitic plant, is specific to sunflower crops. Broomrape seeds perceive their host thanks to germination stimulants present in sunflower root exudates (Bouwmeester et al., 2021). Once germinated, the broomrape radicle grows toward the host root (Krupp et al. 2021) and develops papillae, which adhere to the host root and secrete mucilaginous compounds (Joel and Losner-Goshen, 1994). Subsequently, epidermal cells at the tip of the haustorium, a specific parasitic organ, differentiate into intrusive cells that penetrate the host root (Masumoto et al., 2021). This penetration combines physical pressure and degradation of sunflower root cell walls thanks to pectolytic activity enzymes released by the parasitic plant (Shomer-Ilan, 1993; Losner-Goshen et al., 1998). Intrusive cells make their way toward the host root vessels, crossing the successive host root tissues. Transcriptomic analyses showed that, in the case of a susceptible interaction, defense genes were activated only transiently and at a low level (Letousey et al., 2007; Dos Santos et al., 2003a, b). In addition, the expression of the putative defense suppressor gene *Par1* of various parasitic plants at the early stages of interaction (Yang et al., 2020; Qiu et al., 2022), suggests manipulation of their host by parasitic plants. Once in contact with the host xylem vessels, intrusive cells differentiate into vessel elements and vascular connections are established (xylem as well as phloem), to insure the nutrient supply of the parasite (Krupp et al., 2019). Although numerous studies have been performed on parasitic seed germination and haustorium development (Yoshida et al. 2016), most of them were focused on the parasitic plants, and the host cellular mechanisms involved during the intrusive cell development were poorly described (Mutuku et al., 2021). How the host cells behave during the massive expansion of the haustorium tissues across the outer root cell layers remained quite unknown. A few studies published in the 70-90s explored the host cellular reorganization during the early stages of the haustorium penetration of various *Orobanchaceae* parasitic plant species. It was shown that haustorium development is accompanied by unusual host cell proliferation (Kuijt 1977; Dörr and Kollmann, 1974). Whether the penetration is intra or intercellular in the root host was rarely stated. Dörr and Kollman (1974) and Kuijt (1977) mentioned intercellular growth only of the haustorial cells, with no observations of plasmodesmata interconnecting host and parasite cells for the interactions *O. crenata/ Vicia faba* and *O. ramosa/ Cannabis sativa.* Intercellular penetration between two cortical cells was shown during the interaction between *Striga gesnerioides* (another *Orobanchaceae* species) and cowpea (*Vigna unguiculata;* Reiss and Bailey, 1998). By contrast, the work by Dörr (1969) on the stem parasitic plant species *Cuscuta*

(*Convolvulaceae* family) on the host *Pelargonium zonale* revealed intracellular as well as intercellular penetrations preceding the vascular connection between the host and the parasite (Press et al., 1990). In addition, Musselmann and Dickinson (1975) showed an example of an intrusive cell of the parasitic plant *Agalinis aphylla* (*Orobanchaceae* family) penetrating intracellularly a cortical cell through a small opening in the cell wall. Thus, whether sunflower root penetration by the broomrape haustorium is intra and/or inter cellular remained an open question. This knowledge is required in the perspective of subsequently investigate and understand the sunflower cellular mechanisms associated with resistances to *O. cumana*. In this work, using an efficient selection of the early stages, and combining various microscopy approaches including live-cell imaging of transgenic fluorescent host tissues, we re-investigated the relationships between host and parasitic tissues at the cell level during the early stages of haustorium penetration. The questions we addressed were: *(i)* do intrusive cells penetrate the host root inter or intra-cellularly? *(ii)* do the sunflower root cells in the vicinity of the intrusive cells die or stay alive? *(iii)* are sunflower cell divisions induced at the very early stages of the penetration, and which are the root tissues involved?

Early stage kinetics of the sunflower/ broomrape interaction in rhizotrons

To answer these questions, we needed to observe attachments at very early stages, *i.e.* haustorium penetration sites sampled before the establishment of vessel connections. To this end, we used a dedicated growth and inoculation device called rhizotron, a plexiglass home-made box, which facilitates the observation of inoculated sunflower roots and selection of attachment sites (Le Ru et al., 2021, **Notes S1**). For large field and transmission electron microscopy (TEM) observation of stained longitudinal sections of attachments, we used root fragments from young inoculated wild-type sunflower plantlets (*i.e.* non-transformed). In addition, to get more information on the living status and the sub-cellular organization of the penetrated cells, we observed attachments using *in vivo* confocal imaging of living inoculated transgenic composite sunflower plants, *i.e.* obtained by *Agrobacterium rhizogenes*-mediated transformation. This method generated plants with fluorescent roots, expressing the Green Fluorescent Protein (GFP) targeted to the endoplasmic reticulum (ER) (**Fig. S1**-**S2**; **Table S1**).

Observation of attachments was performed from 4 to 8 days after inoculation (dai) (**Table S2**). Broomrape rarely penetrated the host root before 6 dai, while most of the haustoria had reached the inner root tissues (inner cortex to the vessels) at 8 dai. The kinetics were very similar whatever the type of plants and microscopy approach. Interestingly, similarly to our

observations, Joel and Losner-Goshen (1994) observed the first stages of attachments at 5-7 dai.

Broomrape enters into living sunflower root tissues intracellularly

Germinated broomrape seeds developed papillae at the tip of the radicle when contacting the host root (**Fig. S2i,** Joel and Losner-Goshen, 1994). Mechanical pressure of the broomrape in contact with sunflower root epidermal cells led to cell wall deformation (**Fig. 1a-c**). Differentiated intrusive cells at the broomrape radicle tip were strongly stained by toluidine blue O. They displayed a very dense cytoplasm, a reduced vacuole and a large nucleus containing a darkly stained nucleolus, suggesting a high metabolic activity (**Fig.1a, d, g**, **j**). Imaging early stages of broomrape penetration revealed that intrusive cells penetrated the epidermal layer as well as the successive outer cortical layers intracellularly (**Fig. 1d-i**). In our culture system, sunflower roots had 4 to 5 cortical cell layers between the epidermis and the endodermis (**Fig. S3**). Intracellular penetration of sunflower root cells was observed in all the analyzed penetration sites (21 sites for large field microscopy and 21 sites for confocal microscopy, **Table S2**). The use of the GFP-ER construct provided information about both the cytoplasmic organization and the nucleus position, thanks to the ER outline labelling the nuclear envelope (Genre et al. 2005). In many cases, the nucleus of the penetrated cell was strikingly positioned close to the intrusive cells (**Fig. 1b, c, h, i**). The nucleus re-positioning close to the intruder, is reminiscent of the cellular reorganization of plant cells during bacterial and fungal symbiotic or pathogenic interactions (Fournier et al., 2008; Genre et al., 2005, 2008; Genre et al., 2009). It suggests that the host nucleus perceives the intrusive cell, either through the exerted mechanical pressure (Genre et al. 2009) and/or through unknown chemical signals. However, in contrast to root penetration by symbiotic (Genre et al., 2005; 2008) or pathogenic biotrophic fungi (Koh et al., 2005; Kankanala et al., 2007; Genre et al., 2009), no cytoplasmic aggregation, nor specific ER re-organization were observed ahead of the penetration process. Interestingly, ER was surrounding the broomrape intrusive cells (**Fig. 1e, f, h, i, k, l**), showing active, though not massive, host intracellular re-organization along with the penetration process. These results suggested active membrane synthesis around intrusive cells requiring nucleus and ER activity in the host cell, and showed that the sunflower penetrated cells remained alive. Deeper root tissues (endodermis and pericycle) were also penetrated intracellularly by intrusive cells (**Fig. 1j**). In most cases, haustoria penetrated the host root with minimal host cell damage. However, the live-cell imaging approach revealed a few cases of cell death as shown by the absence of fluorescence (2 sites, **Fig. S4a, b**), or a severe ER disruption

(1 site, **Fig. S4c, d**). Similarly, change of the vacuole structure was observed using large field microscopy for a few sites (7 sites among 21 penetration sites): appearing as a blue smear (**Fig. 1d; Fig. S4e**) or light blue material filling the cell (**Fig. S4e**). One or a few penetrated cells only were affected, adjacent to the intrusive cells in outer root tissues. These results suggested that in some cases, penetration of the intrusive cells got out of control and synchronization of the penetration process and the sunflower cellular re-organization failed, leading to sunflower cell death. This phenomenon remained cell-autonomous, without other defense reactions in the surrounding or the deepest root tissues. Furthermore, penetration could result in the separation of the host nucleus from the distal part of the penetrated cell, probably leading to cell death as well. Strikingly, broomrape intrusion was thicker in outer root tissues (**Fig. 1)** than in inner root tissues, in which only single elongated and separated intrusive cells were detected (**Fig. 1e, f, h, i, k, l**). Similarly, Dörr et al. (1969) reported intracellular "searching hyphae" for the *Cuscuta* stem parasite.

Divisions are induced at very early stages

Sunflower roots were known to swell locally at the site of broomrape attachment by means of cell division (Kuijt, 1977) and as early as 7 dai (Dörr and Kollamnn, 1994). In the present study, sunflower root cell divisions were observed as early as 6 dai, close to attachments (respectively 9 and 7 sites for sections and live-cell imaging). Divisions were mostly anticlinal in the cortex, and periclinal in the pericycle (**Fig. S5; Fig. 1d, e, h, i**). The number of dividing root cell layers and the length of the dividing zone were highly variable (for example from 1 cortical cell to more than 30 cells in a row). These divisions may account for root hypertrophy that was previously observed at the site of 14-dai attachments in rhizotrons (Chabaud et al., 2022). These divisions could be induced indirectly (host hormonal regulation) or directly by the parasitic plant (hormonal release: such as auxin [Ishida et al., 2016] or cytokinin [Spallek et al., 2017]). Whether germinated broomrape seed exudates would be sufficient for the induction of host cell divisions remains an open question.

Intrusive cells penetrate a new apoplastic compartment

The interface between intrusive cells and the sunflower penetrated root cells at early stages of the interaction was further characterized by TEM (**Fig. 2)**. A 7 dai attachment with the haustorium reaching the 3rd cortical cell layer is illustrated **Fig. 2a, b**. Starch grains, a sign of the transition from the autonomous (germination stage) to the parasitical stage (Joel and Losner-Goshen, 1993), were present in the central part of the attachment (**Fig. 2a, c**). In the outer root cell layers, the interface appears as a thick layer surrounding broomrape (**Fig. 2b**), as already

described for *Striga* (Reiss and Bailey, 1998; Neuman et al., 1999). The intrusive cells were easily distinguished from sunflower root cortical cells thanks to their dense cytoplasm, containing Golgi stacks, large mitochondria as well as a reduced vacuole (**Fig. 2b, e, f**) as already reported by Kuijt and Toth (1976) and Kuijt (1977). By contrast, the host cortical cells whether penetrated or not, contained a large vacuole with a thin layer of surrounding cytoplasm (**Fig. 2b, d**). Mitochondria in the penetrated host cells were present all along the host plasmalemma, suggesting intense activity at the periphery of the host cell such as membrane biosynthesis (**Fig. 2d)**. This dense cytoplasm confirmed that the penetrated host cells were alive at this stage. The parasitic cell wall was present all around the intrusive cells. By contrast, the presence of a host matrix along the anticlinal interface of the host penetrated cell was not always detectable and its appearance varied along the length of the haustorium. On the outermost anticlinal side of the host penetrated cell, the host interface with the haustorium appeared as a dark thick layer, in continuity with the existing periclinal host cell wall (**Fig. 2b, d**). It could partly result from the invagination of the existing periclinal host cell wall pushed in by the penetrating intrusive cells. The discontinuity of the staining suggests disorganization of this host cell wall/ matrix. On the innermost side of the cell, the host matrix was either too thin to be visible (**Fig. 2e, f**) or appeared as a low-density material **(**stars in **Fig 2. g, h**) separating the host cell plasmalemma from the parasitic cell wall, and differing from the existing darker periclinal host cell wall. The use of various fluorescent dyes to distinguish host cell wall from newly-made matrix would be interesting, as done for the symbiotic nitrogen-fixing bacterial infection thread (Rae et al., 2021). At the frontline of the haustorium penetration the existing periclinal host cell wall seemed also disorganized (**Fig. 2i**), suggesting progressive local enzymatic degradation of the host cell wall. This apparent dissolution of the nearby host cell walls (Kuijt, 1977) or a partial digestion of the cell wall at the interface (Kurotani et al., 2020, in the case of the interaction *Ptheirospermum japonicum*/ *Arabidopsis thaliana*) had been reported previously. While cell-wall degrading enzymes which might contribute to this process have been identified from the parasite (Shomer-Ilan et al., 1993; Loshen-Gosner et al., 1998), there is no evidence at the moment of the direct involvement of host enzyme activities involved in host cell wall degradation in this context (Mitsumatsu et al., 2015; Yang et al., 2020). Nevertheless, the host cell plasmalemma seemed to remain undisturbed and continuous (**Fig. 2g; Fig. S6b**). Both host and parasitic plasma membranes were highly convoluted at the front line of the haustorium (**Fig. S6b)**, suggesting membrane synthesis for the haustorium accommodation (host) and haustorium expansion (parasite). No plasmodesmata were observed on the interface at these early stages, indicating that molecular exchanges between the parasite

and the host happened at later stages, or through vessel connections, as interspecific plasmodesmata have been shown in the phloem (Krupp et al., 2019). In some cases, the penetration led to disaggregation of the vacuole of the host cell (**Fig. S6c-d**), with disruption of the host cell plasmalemma, leading to cell necrosis, as for *Striga* (Neuman et al., 1999). However as mentioned above this was not very common and remained cell autonomous. In addition, no evidence of cell death was observed at the later stages (Chabaud et al., 2022). Altogether, these results showed that the parasitic intrusive cells penetrate the host root cells intracellularly, as a result of degradation of the host cell wall and formation of a new host trans-cellular apoplastic compartment for haustorium accommodation.

Concluding remarks

Most striking among our findings has been the observation of intracellular haustorium penetration of host root tissues, in contrast to most studies on *Orobanchaceae*. These studies relied mainly on the observation of transverse sections, by contrast to the longitudinal sections used in this work, which made it easier to distinguish between intra and intercellular processes. Our work showed the intimate broomrape penetration into its host, through the formation of a new apoplastic compartment. It suggested that although host cell wall integrity has been damaged by parasitic cell wall degrading enzymes (Shomer-Ilan et al., 1993; Losner-Goshen et al., 1998), only minor defense reactions were induced as previously reported for biotrophic pathogenic fungi (Mendgen and Hahn, 2002; Bellincampi et al., 2014). In that respect, genes encoding inhibitors of cell wall degrading enzymes could be good candidates for increasing resistance to broomrape. In addition, as *HaOr7* (Duriez et al. 2019) and $HaOr_{Deb2}$ (Fernandez-Aparicio et al., 2022) encode Leucine-Rich-Repeat Receptors Like Proteins, providing resistance to various *O. cumana* races, it would be of outstanding interest to characterize the cellular processes involved in these incompatible interactions. Comparing the cellular processes for various *O. cumana* races could highlight common or different mechanisms. Finally, using these approaches on other major parasitic plant species such as *Striga* will be of great interest for future resistance development in a larger host range.

Acknowledgments

We thank P. Gresshoff (University of Queensland, Australia) for the *A. rhizogenes* strain K599. This study was supported by the “Laboratoires d’Excellences (LABEX)” “Towards a Unified theory of biotic interactions: roLe of environmental Pertubations” (TULIP; ANR-10-LABX-

41)" and/or by the "École Universitaire de Recherche (EUR)" TULIP-GS (ANR-18-EURE-0019). Slide scanning was performed using the Nanozoomer from the Imagery Platform of the Federated Research Institute AgroBiosciences-Interactions-Biodiversité (FRAIB; Castanet-Tolosan, France). This study was performed in the frame of a 2-year project (SunOrCell), funded by "Promosol/ SeleoPro" (the association of French Sunflower and Rapeseed Breeders for promoting these crops). The International Consortium of Sunflower Genomics (ICSG) supported the grants for the training students CG and ARS.

Competing interests

None.

Authors and contribution

MCA performed cytological experiments (large field microscopy and TEM). CG, ARS and AL established sunflower transformation experiments. MCB produced sunflower and broomrape resources. SM: coordinated the ICSG, assisted with the construction of the project and the writing of the manuscript. JF gave technical and scientific advice, assisted with the construction and the writing of the manuscript. MC designed the experiments, carried out confocal microscopy and cytology experiments, wrote the manuscript.

ORCID

Mireille Chabaud: https://orcid.org/0000-0002-7786-6895

Joëlle Fournier : https://orcid.org/0000-0003-3746-8080

Stéphane Muños: https://orcid.org/0000-0003-0261-2759

Data availability statement

The original contributions presented in the study are included in the article/Supplementary Material. Further inquiries can be directed to the corresponding author.

References

Bellincampi D, Cervone F, Lionetti V. 2014. Plant cell wall dynamics and wall-related susceptibility in plant-pathogen interactions. *Frontiers in Plant Science* **5**: 228.

BouwmeesterH, Li C, Thiombiano B, Rahmini M, Dong L. 2021. Adaptation of the parasitic plant lifecycle: germination is controlled by essential host signaling molecules. *Plant Physiology* **185**: 1292-1308.

Chabaud M, Auriac M-C, Boniface M-C, Delgrange S, Folletti T, Jardinaud M-F, Legendre A, Perez-Vich B, Pouvreau J-B, Velasco L, Delavault P, Muños S. 2022. Wild *Helianthus* species: A reservoir of resistance genes for sustainable pyramidal resistance to broomrape in sunflower. *Frontiers in Plant Science* **13**.

Dörr I. 1969. Feinstruktur intrazellular wachsender Cuscuta-Hyphen? *Protoplasma* **67:** 123-137.

Dörr I, Kollmann R. 1974. Strukturelle Grundlage des Parasitismus bei *Orobanche* I. Wachstum der Haustorialzellen im Wirtsgewebe. *Protoplasma* **80**: 245-279.

Dos Santos CV, Delavault P, Letousey P, Thalouarn P. 2003a. Identification by suppression subtractive hybridization and expression analysis of Arabidopsis thaliana putative defence genes during Orobanche ramosa infection *Physiology Molecular Plant Pathoogyl* **62**: 297–303.

Dos Santos CV, Letousey P, Delavault P, Thalouarn P. 2003b. Defense Gene Expression Analysis of *Arabidopsis thaliana* Parasitized by *Orobanche ramosa*. *Phytopathology* **93**: 451-457.

Duriez P, Vautrin S, Auriac MC, Bazerque J, Boniface MC, Callot C, Cauet S, Chabaud M, Gentoux F, Lopez-Sendon M et al. 2019. A receptor-like kinase enhances sunflower resistance to *Orobanche cumana*. *Nature Plants* **5**: 1211-1215.

Fernandez-Aparicio M, del Moral L, Muños S, Velasco L, Pérez-Vich B. 2022. Genetic and physiological characterization of sunfower resistance provided by the wild-derived Or_{Deb2} gene against highly virulent races of *Orobanche cumana* Wallr. *Theoritical Applied Genetics* **135** : 501-525

Genre A, Chabaud M, Timmers ACJ, Bonfante P, Barker DG. 2005. Arbuscular mycorrhizal fungi elicit a novel intracellular apparatus in Medicago truncatula root epidermal cells before infection. *Plant Cell* **17**: 3489-3499.

Genre A, Chabaud M, Faccio A, Barker DG, Bonfante P. 2008. Prepenetration apparatus assembly precedes and predicts the colonization patterns of arbuscular mycorrhizal fungi within the root cortex of both *Medicago truncatula* and *Daucus carota*. *Plant Cell* **20**: 1407-1420.

Genre A, Ortu G, Bertoldo C, Martino E, Bonfante P. 2009. Biotic and abiotic stimulation of root epidermal cells reveals common and specific responses to arbuscular mycorrhizal fungi. *Plant Physiology* **149**: 1424-1434.

Ishida JK, Wakatake T, Yoshida S, Takebayashi Y, Kashara H, Wafula E, dePamphilis CW, Namba S, Shirasu K. 2016. Local auxin biosynthesis mediated by a YUCCA flavin monooxygenase regulates haustorium development in the parasitic plant *Phtheirospermum japonicum*. *Plant Cell* **28**: 1795-1814.

Joel DM, Losner-Goshen D. 1994. The attachment organ of the parasitic angiosperms *Orobanche cumana* and *O. aegyptiaca* and its development. *Canadian Journal Botany* **72**: 564-574.

Kankanala P, Czymmek K, Valent B. 2007. Roles for rice membrane dynamics and plasmodesmata during biotrophic invasion by the blast fungus. *Plant Cell*. **19**: 706-724.

Koh S, Andrea A, Edwards H, Ehrhardt D, Somerville S. 2005. *Arabidopsis thalinan* subcellular responses to compatible *Erysiphe cichoracearum* infections. *Plant Journal* **44**:516-529.

Krupp A, Heller A, Spring O. 2019. Development of phloem connexion between the parasitic plant *Orobanche cumana* and its host sunflower. *Protoplasma* **256:** 1385-1397.

Krupp A, Bertsch B, Spring O. 2021. Costunolide Influences Germ Tube Orientation in Sunflower Broomrape - A First Step Toward Understanding Chemotropism. *Frontiers in Plant Science* **12**.

Kuijt J. 1977. Haustoria of phanerogamic parasites. *Annual Review Phytopathology* **17:** 91-118.

Kuijt J, Toth R. 1976. Ultrastructure of angiosperm haustoria-A review. *Annals Botany* **40**: 1121-30.

Kurotani KI, Wakatake T, Ichihashi Y, Okayasu K, Sawai Y, ogawa S, Cui S, Suzuki T, Shirasu K, notaguchi M. 2020. Host-parasite tissue adhesion by a secreted type of beta-1,4-glucanase in the parasitic plant *Phtheirospermum japonicum*. *Communications Biology* **3**.

Le Ru A, Ibarcq G, Boniface MC, Baussart A, Munos S, Chabaud M. 2021. Image analysis for the automatic phenotyping of *Orobanche cumana* tubercles on sunflower roots. *Plant Methods* **17**.

Letousey P, de Zelicourt A, Dos Santos CV, Thoiron S, Monteau F, Simier P, Thalouarn P, Delavault P. 2007. Molecular analysis of resistance mechanisms to *Orobanche cumana* in sunflower. *Plant Pathology* **56**: 536-546.

Losner-Goshen D, Protnoy VH, Mayer AM, Joel DM. 1998. Pectolytic Activity by the Haustorium of the Parasitic Plant *Orobanche L.*(Orobanchaceae) in Host Roots. *Annals Botany* **81**: 319-326.

Masumoto N, Suzuki Y, Cui S, Wakazaki M, Sato M, Kumaishi K, Shibata A, Furuta K, Ichihashi Y, Shirasu K *et al*. 2021. Three-dimensional reconstructions of haustoria in two parasitic plant species in the Orobanchaceae. *Plant Physiology* **185:** 1429–1442.

Mendgen K, Hahn M. 2002. Plant infection and the establishment of fungal biotrophy. *Trends in Plant Science* **7**: 352-356.

Mitsumasu K,Seto Y, Yoshida S. 2015. Apoplastic interactions between plants and plant-root intruders. *Frontiers in Plant Science* **6:** 617.

Mutuku JM, Cui S, Yoshida S, Shirasu K. 2021. Orobanchaceae parasite–host interactions. *New Phytologist* **230**: 46–59.

Musselman LJ, Dickison WC. 1975. The structure and development of the haustorium in parasitic Scrophulariaceae. *Botanical Journal Linn. Society* **70:** 183-212.

Neumann U, vian B, weber HC, Sallé G. 1999. Interface between haustoria of parasitic members of the Scrophulariaceae and their hosts: a histochemical and immunocytochemical approach. *Protoplasma* **207**: 84-97.

Press MC, Gravest JD, Stewart GR. 1990. Physiology of the interaction of angiosperm parasites and their higher plant hosts. *Plant Cell and Environment* **13:** 91-104.

Qiu S**,Bradley** JM**, Zhang** P**, Chaudhuri** R**, Blaxter** M**, Butlin** RK**, Scholes JD. 2022**. Genome-enabled discovery of candidate virulence loci in *Striga hermonthica*, a devastating parasite of African cereal crops. *New Phytologist* **236**: 622–638.

Rae AE, Rolland V, White RG, Mathesius U. 2021. New methods for confocal imaging of infection threads in crop and model legumes. *Plant Methods* **17:** 24.

Reiss GC, Bailey JA. 1998. *Striga genesrioides* parasiting cowpea: development of infection structures and mechanisms of penetration. *Annals Botant* **81**: 431-440.

Shomer-Ilan A. 1993. Germinating seeds of the root parasite *Orobanche aegyptiaca* Pers. excrete enzymes with carbohydrase activity. *Symbiosis* **15**: 61-70.

Spallek T, Melnyk CW, Wakatake T, Zhang J, Sakamoto Y, Kiba T, Yoshida S, Matsunaga S, Sakakibara H, Shirasu K. 2017. Interspecies hormonal control of host root morphology by parasitic plants. *Proceedings National Academy Science USA* **114**: 5283–5288.

Yang C, Fu F, Zhang N, Wang J, Hu L, Islam F, Bai Q, Yun X, Zhou W. 2020. Transcriptional profiling of underground interaction of two contrasting sunflower cultivars with the root parasitic weed *Orobanche cumana*. *Plant Soil* **450**: 303–321.

Yoshida S, Cui S, Ichihashi Y, Shirasu K. 2016. The Haustorium, a Specialized Invasive Organ in Parasitic Plants. *Annual Review Plant Biology* **67**:643–67.

339 ***Legends***

340 **Fig.1. Broomrape haustorium penetrates the sunflower root tissues intracellularly.**

341 Broomrape attachments (6-7 dai) were observed at the cellular level, using 2 approaches: *(i)*
342 large field microscopy of thin sections of resin-embedded and toluidine blue O-stained
343 attachments (right column, **a, d, g, j)**; *(ii)* confocal microscopy of broomrape-inoculated
344 transgenic fluorescent sunflower roots expressing the GFP targeted to the endoplasmic
345 reticulum (ER) (middle and left columns, **b, c, e, f, h, i, k, l**). Confocal microscopy images show
346 fluorescence alone (combined GFP fluorescence and auto-fluorescence channels, middle
347 column, **b-e-h-k**) or fluorescence with the corresponding bright field image (left column, **c, f,**
348 **i, l**).

349 **a-c.** Deformation of the epidermal cell wall (arrow) due to the mechanical pressure exerted by
350 the haustorium. Re-positioning of the nuclei of the deformed epidermal cells in the vicinity of
351 the haustorium tip (**b.** white arrowheads). **d–i** and **k-l.** Intrusive cells penetrated the root
352 epidermal and cortical layers intracellularly. The penetrated cortical cells had wavy (**d.** black
353 double arrowheads) or deformed (**g.** black arrow) cell wall in contact with the haustorium. ER
354 surrounded the intrusive haustorium tip (**h, k.** white double arrowheads). Nuclei were
355 positioned close to the intrusive cells (**h.** white arrowheads). **j.** Intrusive cells reached the host
356 xylem vessels (xylem: black cross), and crossed intracellularly the deepest cortical cell layer as
357 well as the endodermis and the pericycle. Divisions in the cortex (mostly anticlinal, squares)
358 and the pericycle (mostly periclinal, double squares) in the vicinity of the haustorium (**d, e, j)**.
359 **c, f, i, l.** White dots outline the broomape haustorium visible on the bright field image. **b-c, e-f**
360 **, k-l** are z axis projections of serial optical sections.

361 Scale bar = 50 µm (**a, b, c, d, e, f, g, j**); 20 µm (**h, i, k, l**).

362

363 **Fig.2. Creation of a new apoplastic compartment for haustorium accommodation.**

364 A 7 dai attachment, with intrusive cells reaching the 3rd cortical cell layer was imaged. **a.**
365 General view of the attachment using large field microscopy. **b-i**. Transmission electron
366 microscopy. IC intrusive cell, HC host cell.

367 **a, b.** Intrusive cells intracellular penetration in the host outer cortex cell. A thick stained layer
368 surrounded the penetrating intrusive cells in outer host tissues (epidermis and outer cortex;
369 black arrows in **a**, red arrows in **b**). **c.** Magnification of the central part of the broomrape, with
370 starch grain-containing cells. **d.** In the outermost side of the anticlinal interface between the
371 intrusive cell and the penetrated host outer cortical cell, disorganization of the host cell

wall/matrix (star). Continuous thin layer of cytoplasm in the host cortical cell (black arrowheads), containing numerous mitochondria (double arrowheads). **e, f**. Presence of the parasitic cell wall but no visible host cell matrix in the outermost anticlinal side of the penetrated cell. **e**. Magnification of **b**. **f.** Magnification of **e. f.** The intrusive cell cytoplasm contains Golgi (thin arrow) and mitochondria (arrowhead). Mitochondria are also present in the thin host cytoplasm layer (double arrowhead). **g-h.** At the tip of the haustorium, presence of a host matrix (star) with fibrillae fragments. Convolution of the plasmalemma of the host cortical cells adjacent to the intrusive cells. **i**. At the front line of the intrusive cell tips (periclinal interface), local disorganization of the host cell wall (star), the plasmalemma of the host cell remaining intact and continuous. The dotted line shows the separation between the parasitic and host cell walls (**g-i**).

Scale bar = 50 µm (**a**); 5 µm (**b**); 10 µm (**c**); 2 µm (**d-e**); 0.5 µm (**f, g, h, i**).

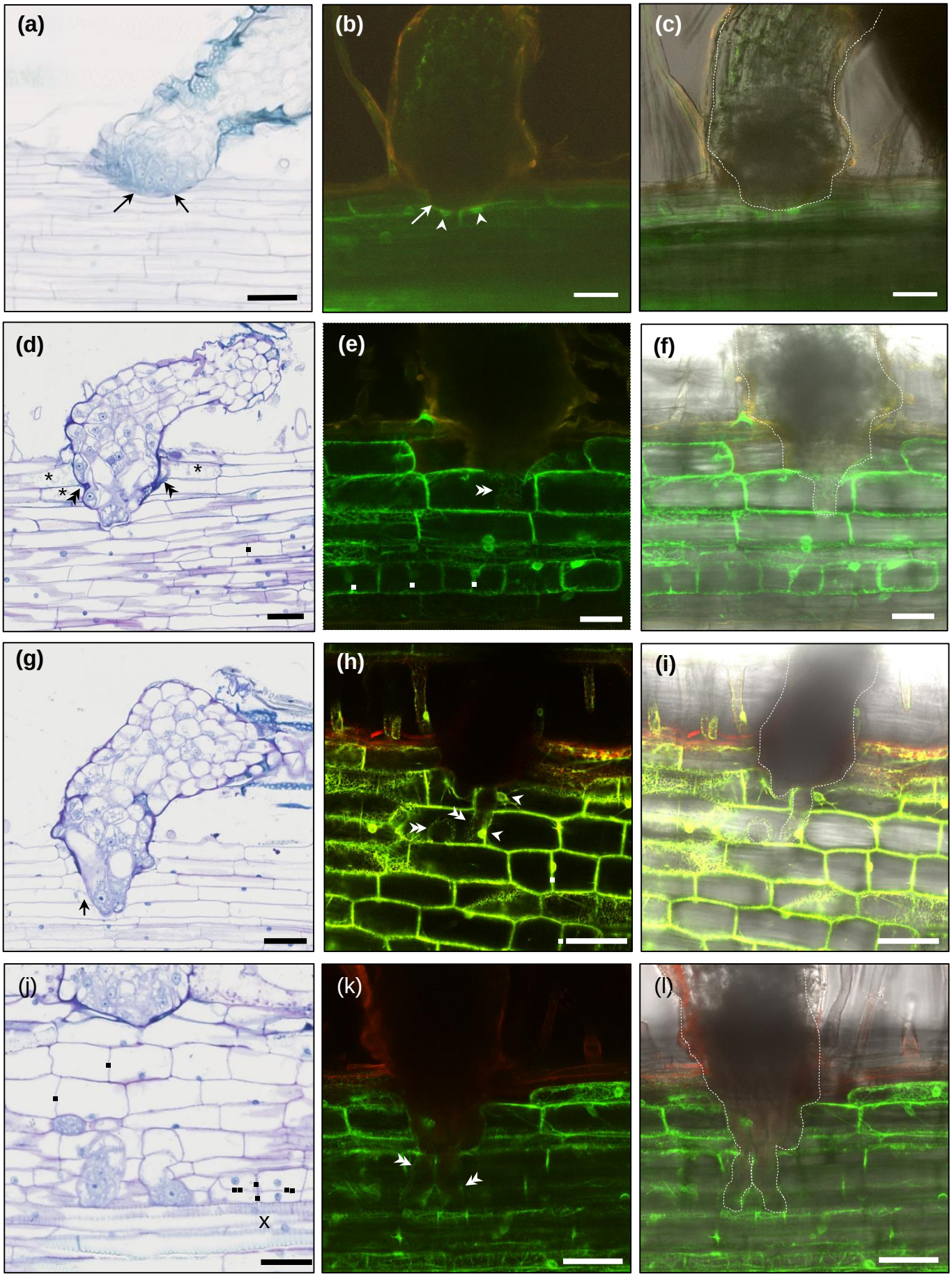
(a)
(b)
(c)
(d)
(e)
(f)
(g)
(h)
(i)
(j)
X
(k)
(l)

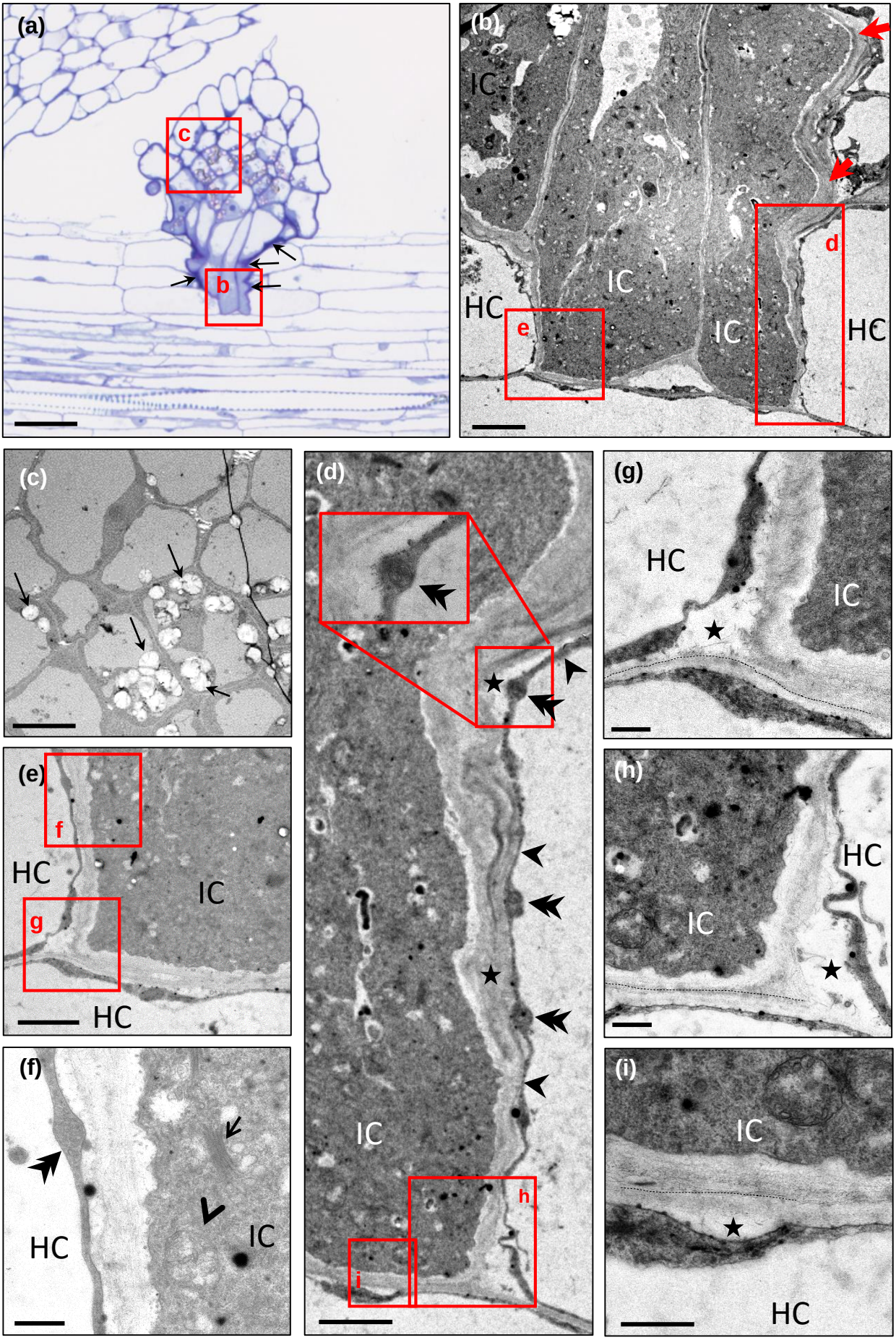
(a)
c
b
(b)
IC
IC
IC
HC
HC
HC
e
d
(c)
(d)
(g)
HC
IC
(e)
f
HC
IC
g
HC
(h)
HC
IC
(f)
HC
IC
IC
h
i
(i)
IC
HC

Notes S1. Details of the materials and methods.

Plant genotypes, bacterial strains, and constructs

We used the susceptible cultivated *H. annuus* L., XRQ (Chabaud et al., 2022; Badouin et al., 2017) as the sunflower host for experiments in rhizotrons and for root transformation experiments. The *O. cumana* Wallr. population used in this study was the French race E-BOU of *O. cumana,* with a virulence level classified between E and F, and harvested in 2017 in Bourret (Tarn et Garonne, France; reference: LIPM-20734).

The *Agrobacterium rhizogenes* strain K599 (Savka et al. 1990) was used for sunflower root transformation. The binary vector used was derived from pBIN19 (Bevan, 1984) and carried the construct p35S-GFP-ER coding for the Cauliflower Mosaic Virus 35S promoter (p35S) driving the constitutive expression of the Green Fluorescent Protein targeted to the endoplasmic reticulum due to the presence of ER-targeting sequences (N-terminal signal peptide) and ER-retention (C-terminal tetra-peptide HDEL; Haseloff et al. 1997). Bacteria were grown on LB medium supplemented with Streptomycin 100 mg/l (bacterial selection) and kanamycin 50 mg/l (plasmid selection)

Cultivation of sunflower plants in rhizotrons

Two types of sunflower plants were used: wild-type (non-transformed, non-fluorescent) sunflower plantlets for large field and TEM microscopy, and transgenic composite plants (expressing the fluorescent marker in their roots only) for confocal microscopy.

Wild-type (*i.e.* non-transformed) sunflower plants

Sunflower seeds of wild-type plants were surface sterilized for 10 min in a 4.8 % sodium hypochlorite solution, rinsed 3 times and sown in a 1/1 v/v mixture of sand/ vermiculite in alveoli. Seedlings were grown at 22 °C, 60% humidity, 16 h light 118 µE/m²/s for 7 days. Rhizotrons, 12x12 cm home-made plexiglass boxes were assembled as described in Le Ru et al. (2021), with water-soaked sterile rock-wool, a sterile glass fiber paper and a 7-day old sunflower plantlet. Rhizotrons were then watered with a ½ Long Ashton solution (Hewitt, 1966) containing 370 µM phosphate.

Transgenic composite sunflower plants

To transform sunflower roots and obtain composite plants (with a non-transformed aerial part and transgenic roots), we used a modified version of the protocol from Parks and Yordanov (2020, **Fig. S1-S2**). Sunflower seeds were decontaminated and grown in alveolus-trays as above for 10 days. Transformation of plantlets was performed in soaked pre-cut rock-wool cubes

(reference ALR02G from GRODAN) with bacterial solution [final OD= 0.25 in ¼ (MS + Gamborg vitamins B5)], in Magenta boxes. After 3 days, Magenta boxes were slightly opened. Six days after transformation, plantlets were transferred to hydroponics, using sterile 1000µl cone boxes, as described in Morel et al. (2018) for another 6 days of culture in ¼ MS liquid medium (without vitamins; Sigma reference MS 5524). Culture in hydroponics, a new step compared to Parks and Yordanov's protocol (2020) was very beneficial to newly developed root growth. Finally, 14 to 18 days following transformation (6-7 days in rock-wool cubes and 7-12 days in hydroponics; **Fig. S1**), transformation efficiency was recorded by measuring the percentage of plants with fluorescent roots and the number of fluorescent roots/ transformed plant (**Table S1**). Fluorescence expression was observed by epifluorescence microscopy using a stereomicroscope (Axiozoom V16; Zeiss), equipped with a GFP Long Pass filter (excitation 485/12 nm and emission from 515 LP). Composite plants were transferred to rhizotrons as for non-transformed plantlets (see above).

Four experiments were performed. In the first experiment, 17-day-old plantlets were used for transformation, and the transfer to rhizotrons was done 18 days later, resulting in large 35-day-old plants that were difficult to handle under the confocal microscope. Hence the length of culture was progressively reduced in the following experiments to 10-day-old plantlets for transformation, culminating with transfer to rhizotrons as soon as 14 days later in experiment No. 4 (**Fig. S1**). The reduction of the age of the plants used for transformation facilitated the manipulation of the composite plants when they were removed from the rock-wool cubes and limited wounding of the transgenic roots. It also facilitated their transfer into rhizotrons and use in confocal microscopy.

Inoculation of sunflower plants in rhizotrons

Broomrape seeds were surface sterilized for 5 min in a 3.2 % sodium hypochlorite solution, rinsed 3 times using a 40 µm cell strainer, and water-conditioned for 7 days in a 50 ml sterile tube at 23 °C in the dark, at a final concentration of 10 mg/ 3 ml of water. Each rhizotron was inoculated with 10 mg (3 ml) of conditioned broomrape seeds.

Seven day-old wild-type plants were inoculated the day of transfer in rhizotron. For transgenic composite plants the day of inoculation varied among the transformation experiments from 1 to 8 days after the transfer in rhizotrons (*i.e.* 27 to 36 days after sunflower sowing; **Figure S1**).

Microscopic observation of young O. cumana attachments

Young wild-type sunflower plantlets were inoculated and used for large field and transmission electron microscopy (TEM) observation of stained longitudinal sections of attachments. Selected composite sunflower plants with fluorescent roots were inoculated and used for *in vivo* confocal microscopy images of attachments.

Large field microscopy observations

This approach was inspired from the work of Xiao et al. (2014) on early symbiotic nodule development. Four to 8 days after inoculation (dai), root samples were prepared for cytological studies as described in Chabaud et al. (2022). Fixed samples were embedded in Technovit 7100 resin (Heraeus Kulzer,Wehrheim, Germany), according to the manufacturer's recommendations. Thin (4-5 µm) sections, longitudinal to both haustorium and host root, were made using a microtome (2040 Reichert Jung), stained in 0.2% toluidine blue for 3 min, mounted in DePeX mounting medium (BDH Laboratories, Poole, England) and scanned using a Nanozoomer (NDP, Hamamatsu).

Transmission electron microscopy (TEM) observations

Samples were prepared as in Cerutti et al. (2017) with some modifications. Five to 7 dai, broomrape attachments on sunflower root fragments were fixed under vacuum for 30 min with 2.5 % glutaraldehyde in 0.1 M sodium cacodylate buffer (pH = 7.2) containing 0.1 % Triton X100, and then at the atmospheric pressure in the same solution without Triton X100, washed in the same cacodylate buffer and post-fixed for one hour at room temperature with 1 % osmium tetroxide (OsO_4) in the same buffer. They were then dehydrated in ethanol series, and embedded in Epon. Thin (1 µm) or ultra-thin (80-90 nm) sections were prepared on UltraCut E ultramicrotome (Reichert-Jung) equipped with a diamond knife (Reichert-Leica, Germany). The histological organization of tissues was observed on thin sections stained in a 1 % borax solution containing 0.2 % methylene blue and 0.1 % toluidine blue, rinsed in water and then in an aqueous solution of 0.07 % basic fuchsin. Ultrastructural observation was done on ultrathin sections stained with uranyless (Delta microscopy, Mauressac France), and lead citrate (delta microscopies, Mauressac France) using the electron microscope Hitachi-7700 (Japan) operating at 80 kV.

Confocal microscopy

This approach was inspired from the cytology work of Genre et al. (2005) for arbuscular mycorrhizal symbiosis studies on *Medicago* and carrot. Six days after broomrape inoculation

(dai) in rhizotrons, inoculated sunflower composite plants were transferred to a 12x12 cm square Petri dish containing 80 ml of solid medium ½ Long Ashton 370 µM phosphate, 3 g/l Phytagel, with the aerial part outside of the dish (**Fig. S2g**). The root system was covered with a gas-permeable plastic film (Lumox Film, Starsted) as described in Fournier et al. (2015). Attachments were imaged with a Leica TCS SP8 AOBS confocal laser scanning microscope equipped with a long-distance 25X HC FLUOTAR (numerical aperture, 0.95) water immersion objective. The 488 nm argon laser line was used to excite GFP and auto-fluorescence. Specific emission windows used for GFP and auto-fluorescence signals were 500 to 550 nm, and 580 to 650 nm, respectively, and emitted fluorescence was false-coloured in green (GFP), and red (auto-fluorescence). The images shown are single confocal sections or maximal projections of selected planes of a z-stack. Images were acquired and projected using Leica confocal software and processed using Leica confocal software.

References

Badouin H, Gouzy J, Grassa, CJ, Murat F, Staton SE, Cottret L, Lelandais-Briere C, Owens GL, Carrere S, Mayjonade B et al. 2017. The sunflower genome provides insights into oil metabolism, flowering and Asterid evolution. *Nature* **546**: 148

Bevan M. 1984. Binary Agrobacterium vectors for plant transformation. *Nuc. Ac. Res* 12:8711–8721

Cerutti A, Jauneau A, Auriac MC, Lauber E, Martinez Y, Chiarenza S, Leonhardt N, Berthomé R, Noël LD. 2017. Immunity at cauliflower hydathodes controls systemic infection by *Xanthomonas campestris pv campestris*. *Plant Physiology* **174**: 700–716.

Chabaud M, Auriac MC , Boniface Mc , Delgrange S , Folletti T , Jardinaud MF , Legendre A, Perez-Vich B, Pouvreau JB , Velasco L , Delavault P, Muños S. 2022. Wild *Helianthus* species: A reservoir of resistance genes for sustainable pyramidal resistance to broomrape in sunflower. *Frontiers in Plant Science* **13**.

Fournier J, Teillet A, Chabaud M, Ivanov S, Genre A, Limpens E, de Carvalho-Niebel F, Barker B. 2015. Remodeling of the Infection Chamber before Infection Thread Formation Reveals a Two-Step Mechanism for Rhizobial Entry into the Host Legume Root Hair. *Plant Physiology* **167** : 1233–1242.

Genre A, Chabaud M, Timmers ACJ, Bonfante P, Barker DG. 2005. Arbuscular mycorrhizal fungi elicit a novel intracellular apparatus in *Medicago truncatula* root epidermal cells before infection. *Plant Cell* **17**: 3489-3499.

Haseloff J, Siemering KR, Prasher DC, Hodge S. 1997. Removal of a cryptic intron and subcellular localization of green fluorescent protein are required to mark transgenic Arabidopsis plants brightly. *Proceedings National Academy Science USA* **94**:2122–2127.

Hewitt EJ. 1966. Sand and water culture methods in the study of plant nutrition. In: Technical communication no.22. 2nd ed. Rev. Commonwealth Agr. Bur., London.

Le Ru A, Ibarcq G, Boniface MC, Baussart A, Munos S, Chabaud M. 2021. Image analysis for the automatic phenotyping of Orobanche cumana tubercles on sunflower roots. *Plant Methods* **17**.

Morel A, Peeters N, Vailleau, F, Barberis P, Jiang G, Berthomé R, Guidot A . 2018. Plant pathogenicity phenotyping of *Ralstonia solanacearum* strains. In: Medina C Lopez-Baena FJ, eds. *Host-Pathogen interactions: Methods and Protocols*. **1734**: 223-239.

Parks T, Yordanov YS. 2020. Composite plants for a composite plant: An efficient protocol for root studies in the sunflower using composite plants approach. *Plant Cell Tissue and Organ Culture* **140**: 647-659.

Savka M., Ravillion B., Noe, G., Farrand S.1990. Induction of hairy roots on cultivated soybean genotypes and their use to prop-agate the soybean cyst nematode. *Phytopathology*.**80**: 503–508.

Xiao TT, Schilderink S, Moling S, Deinum EE, Kondorosi E, Franssen H, Kulikova O, Niebel A, Bisseling T. 2014. Fate map of *Medicago truncatula* root nodules. *Development* **141**: 3517-3528.

Fig. S1. Sunflower transformation experiments and broomrape inoculation of composite plants for confocal microscopy observations.

The initial experiment (No.1) led to broomrape inoculation of 36-day-old sunflower plants, which were very developed and not easy to handle under confocal microscopy. Hence, the length of culture was progressively reduced in the following experiments to finally reach broomrape inoculation of smaller, 26-day-old plantlets in experiment No.4. This also allowed to generate two series of inoculated plants according to their development in experiments No. 2 and 4, using the most developed composite plants for the 1st inoculation and the less developed composite plants for a 2nd, delayed inoculation 6 days later. Confocal microscopy was performed 5 to 8 dai.

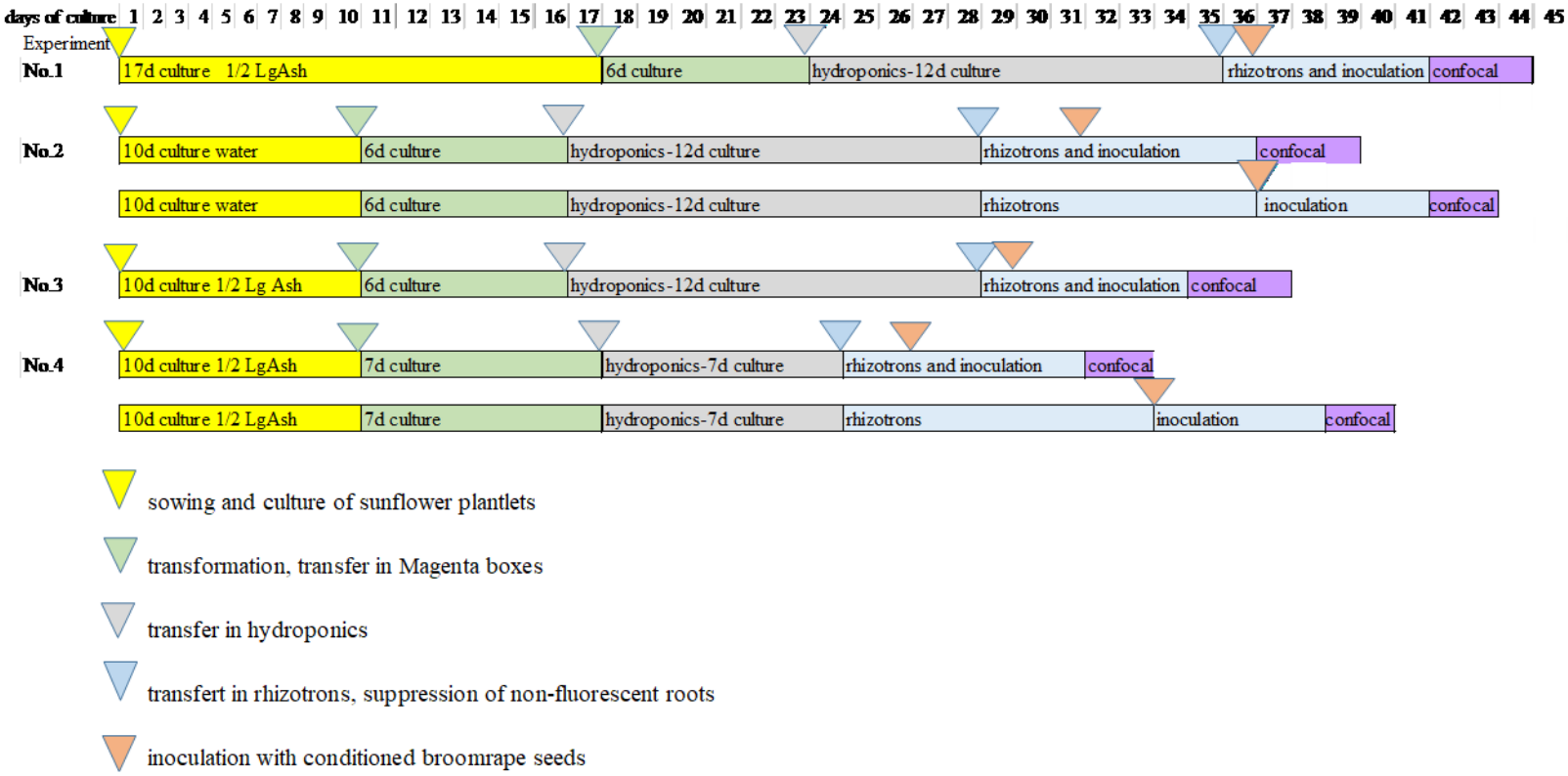

Fig. S2. Transformation of sunflower plants *via A. rhizogenes* and transfer of composite plants in rhizotrons for broomrape inoculation and observation using confocal microscopy.

Cuttings without cotyledons were excised from 10-day-old plantlets (**a**), and transformed in pre-soaked rock-wool cubes with *A. rhizogenes* solution (**b**). Six days later, plantlets were transferred in hydroponics (**c**) for another 8 days of culture. Fourteen days after transformation, green fluorescent transgenic roots were counted under a binocular microscope (**d, Table S1**). Non-fluorescent roots were removed and composite plants were transferred to rhizotrons (**e**) and inoculated with pre-conditioned broomrape seeds 1 to 2 days later (**f**). Five to 8 days after inoculation, inoculated composite plants were transferred to a Petri dish (**g**- 5 dai) and attachments were selected and imaged by confocal microscopy (**h-i**). **i.** Papillae development (arrows). Scale bar = 4 cm (**a**); 2 cm (**b**); 5 cm (**c**); 0.5 cm (**d**); 3 cm (**e-g**); 100 µm (**h**); 10 µm (**i**).

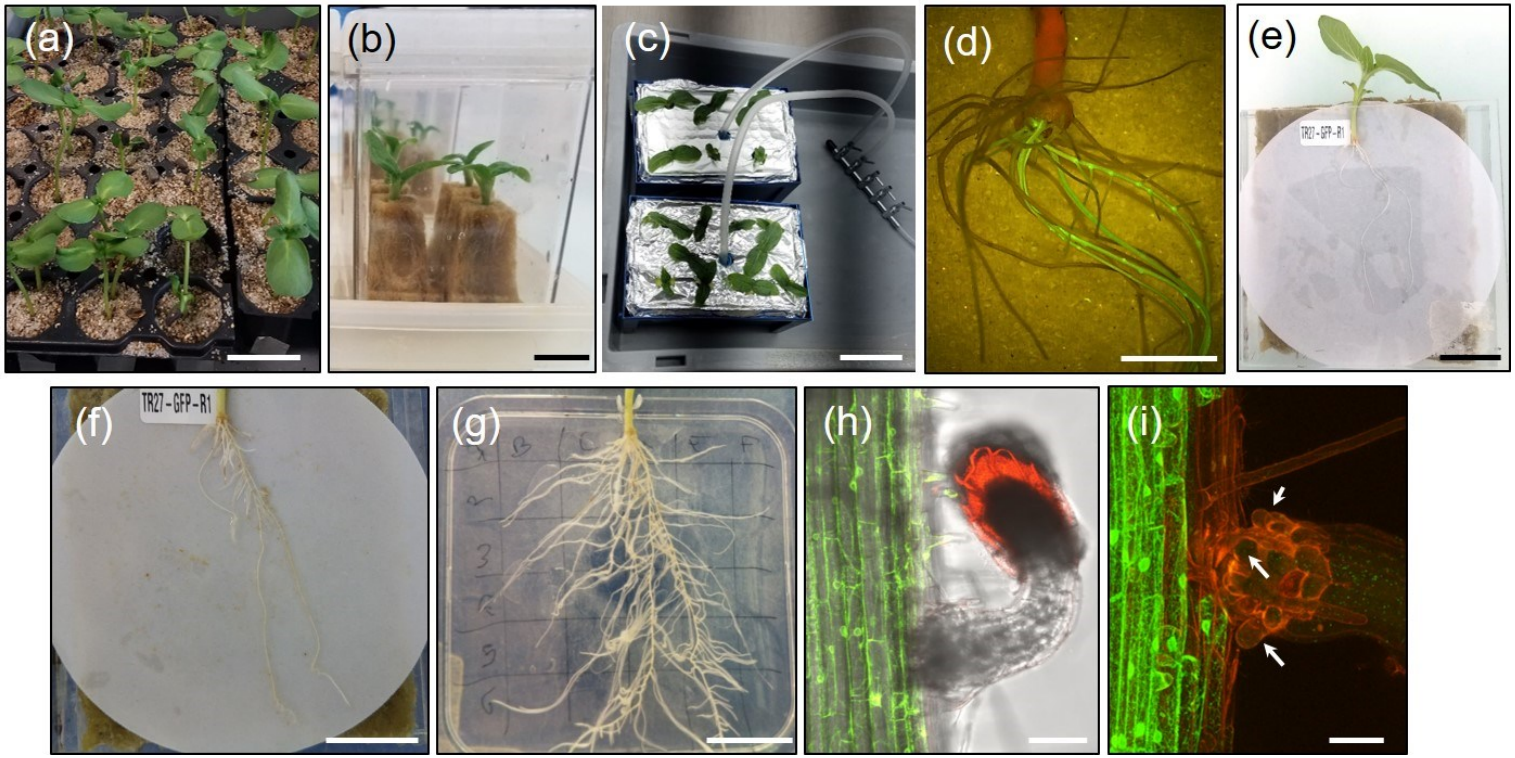

Fig. S3. Longitudinal section of a sunflower root.

A thin section of a sunflower root fragment, without broomrape attachment, resin-embedded and stained with toluidine blue O, was observed using large field microscopy. In our growth conditions, roots displayed 4 to 5 cortical layers.

Scale bar = 100 µm.

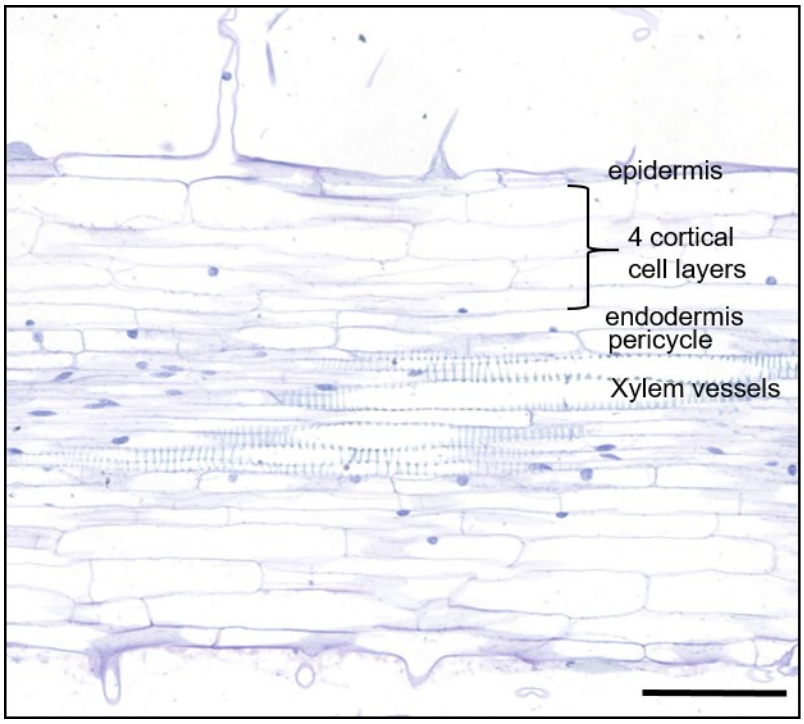

Fig. S4. Cell death or ER de-structuring associated with haustorium penetration.

Confocal microscopy imaging revealed that occasionally, sunflower cells in the vicinity of haustoria cells were either devoid of fluorecence (**a, b**, star) or showed a destructured ER (**c, d**, asterisk), suggesting cell death. **e.** Using bright field microscopy, similar events were observed as destructuring of the vacuole (blue smear, asterisk) or light blue material filling the cell (star). These observations suggested rare occurrence of dying or dead cells in contact or in the vicinity of the haustorium.

Scale bar = 10 µm (**a, b)**; 50 µm (**c-e).**

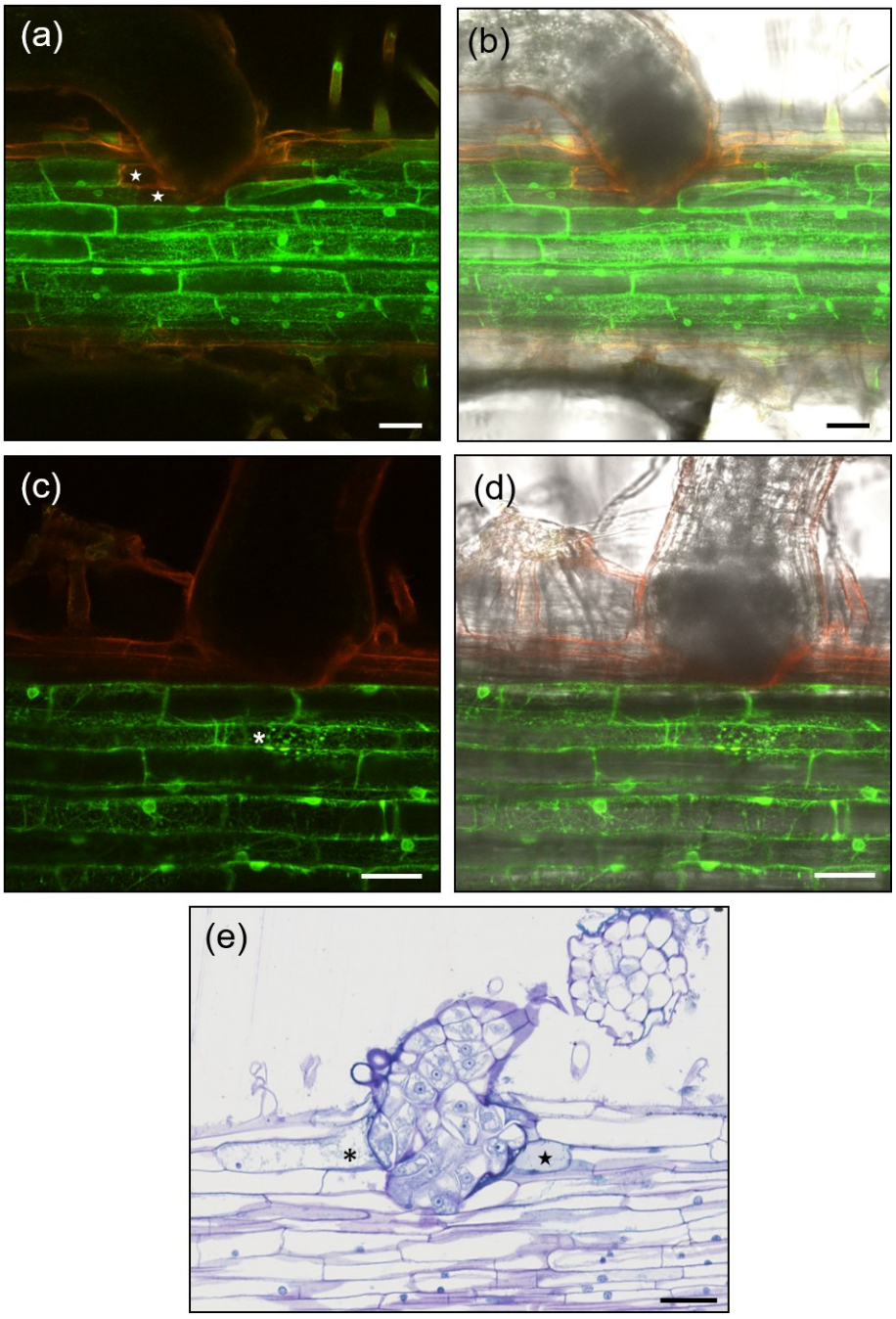

Fig. S5. Multiple divisions in the host root at the site of broomrape intrusion.

Lower magnification image of the section in **Fig. 1j,** showing a wider zone of the root. Cell division was observed around the intrusive cells (arrowheads). Anticlinal divisions affected the host cortex on both sides of the root (black square brackets). Periclinal divisions were visible in the pericycle (red square brackets).

Scale bar = 100 µm.

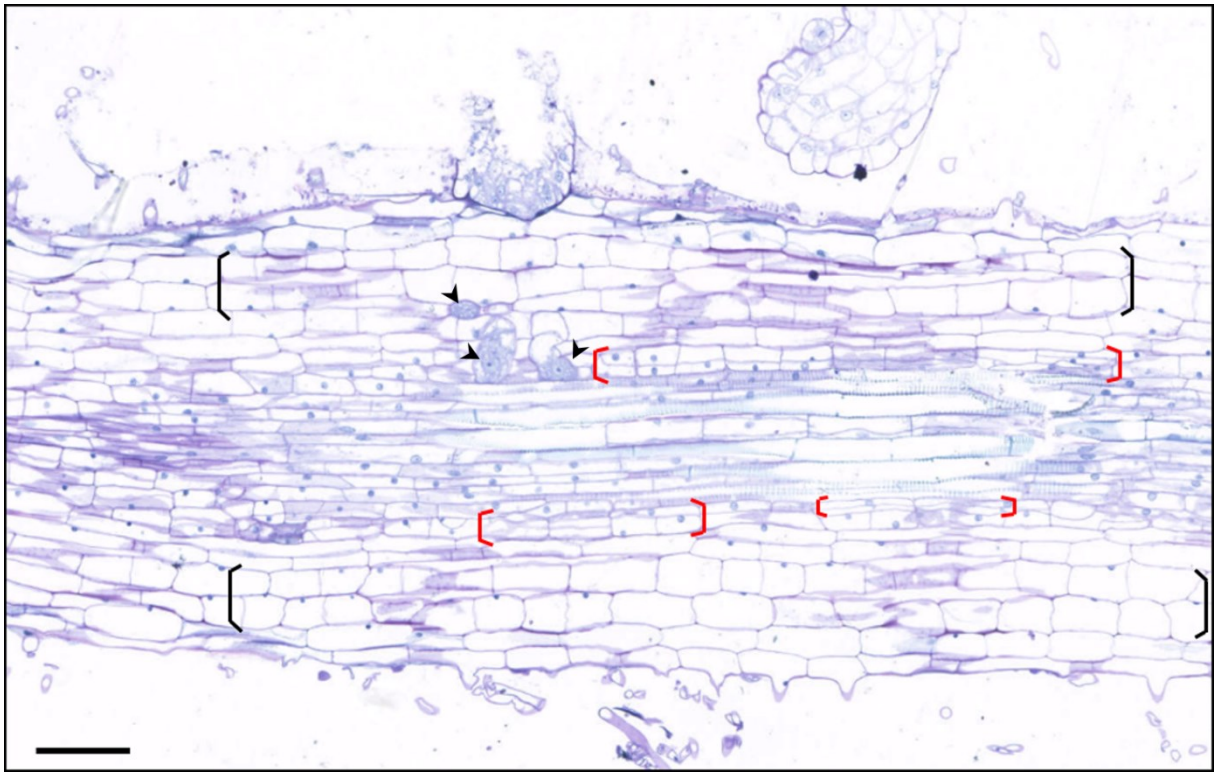

Fig. S6. Transmission electron microscopy of a 7 dai attachment.

The attachment shown in Fig. 2 was sectioned *c.* 9 µm further. **a.** General view of the attachment using large field microscopy. **b-d.** TEM.

a. Intrusive cells showed a dense cytoplasmic content and a big nucleus (arrow), containing a large nucleolus (dark blue). **b.** Assembly of 3 TEM pictures at the interface of the penetrating intrusive cells. The periclinal cell wall of the host cortical cell contacted by the tip of the haustorium was deformed (stars), potentially digested by parasitic pectolytic enzymes. By contrast the parasitic cell wall surrounding the intrusive cells (dotted line) appeared intact and continuous. The plasmalemma of the host cell showed convolution, suggesting active membrane synthesis, preparing the apoplastic compartment for subsequent accommodation of the haustorium. Electron dense granules were present along the host plasmalemma. **c, d**. One of the penetrated cortical cells, adjacent to the attachment, showed abnormal accumulation of granular material inside the vacuole. Electron microscopy of this cell indicated disruption of the tonoplast and plasmalemma as well as cytoplasm degradation, likely causes of cell death. Scale bar = 50 µm (**a**); 5 µm (**b**); 1 µm (**c-d**).

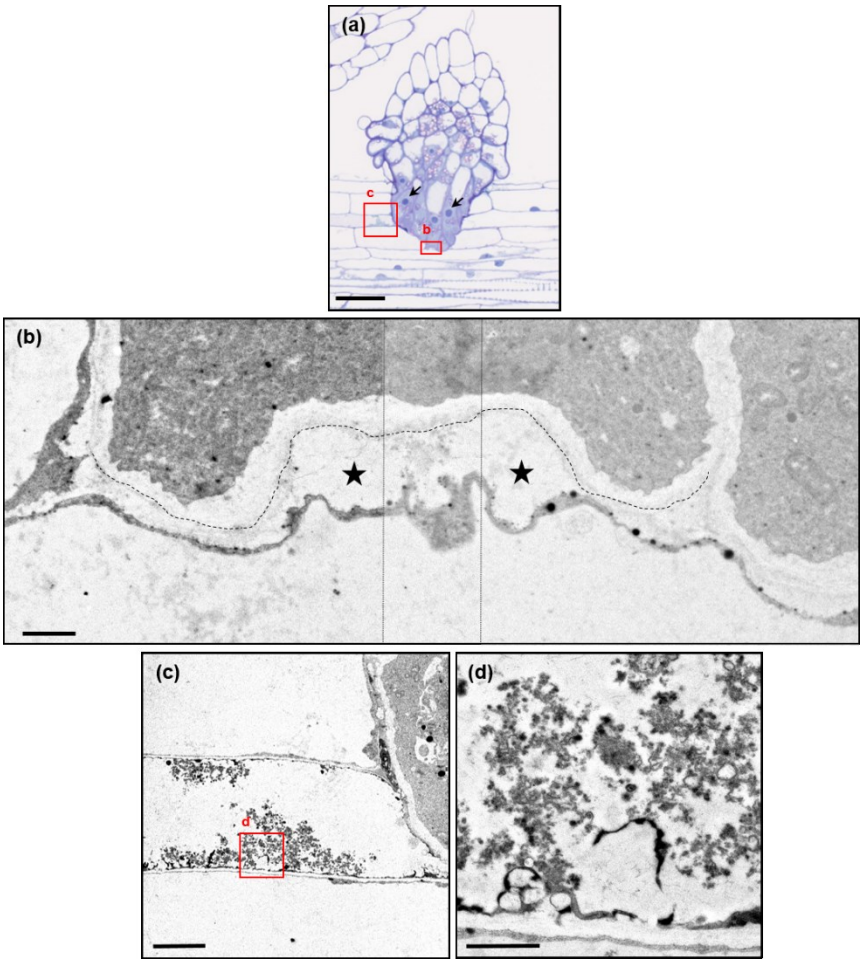

Table S1. Efficiency of sunflower transformation *via A. rhizogenes.*

Four experiments of sunflower transformation were performed, using the p35S-GFP-ER construct (**Fig. S1**). Transgenic fluorescent roots were observed using a stereomicroscope equipped with a Long Pass GFP filter, which allowed to discriminate transgenic green roots from non-transformed orange auto-fluorescent roots. Plants were counted as transformed when at least one green fluorescent root had developed.

NA: data not available. In experiment No.1, composite plants were too developed and consequently transgenic roots were intermingled and difficult to distinguish from one another.

experiment	number of plants	% of transformed plants	number of fluorescent root/ transformed plant	% of fluorescent root/ transformed plant
No.1	20	95	NA	NA
No.2	7	86	4,6	63
No.3	9	100	5,4	51
No.4	10	100	4,9	49

Table S2. Overview of observed sites.

Twenty five attachments (4 to 8 dai) from inoculated wild-type (non transformed) sunflower plants were scored using large field microscopy: 21 sites of penetration and 4 sites without penetration yet. Thirty eight attachments (5 to 7 dai) were scored under confocal microscopy on inoculated transgenic composite plants: 21 sites of penetration and 17 sites without penetration yet. Sites are organized according to time of observation (dai) and stage of colonization (*i.e.* deepest sunflower root cell layer reached by the intrusive cells).

		microscopy	
Time	Stage of colonization	large field	confocal
4 dai	no contact	1	
	epidermis	1	
5 dai	contact but no penetration		3
6 dai	contact but no penetration	3	10
	epidermis	1	1
	1st outer cortex	1	3
	2nd or 3rd outer cortex	1	8
	inner cortex	1	2
	vessels	1	
7 dai	contact but no penetration		4
	epidermis		1
	1st outer cortex	2	2
	2nd/ 3rd outer cortex	4	3
	inner cortex	3	1*
	vessels	1	
8 dai	1st layer outer cortex	2	
	2nd/ 3rd outer cortex		
	inner cortex	1	
	endodermis	1	
	vessels	1	
	total number of sites	25	38

*: inner cortex or deeper